Comparison of Fragmentation Measurements by Photographic and Image Analysis Techniques

Article *in* Rock Mechanics and Rock Engineering · January 2006

DOI: 10.1007/s00603-005-0044-9

3 authors, including:

Govind Raj Adhikari

50 PUBLICATIONS **524** CITATIONS

SEE PROFILE

Rock Mech. Rock Engng. (1999) 32 (4), 291–301

Rock Mechanics and Rock Engineering

Studies on Flyrock at Limestone Quarries

By

G. R. Adhikari

National Institute of Rock Mechanics, Kolar Gold Fields, India

Summary

Observed flyrock distances for 47 blasts at six limestone quarries along with blast design parameters are presented. The influence of blasthole diameter, burden, stemming length, powder factor, the condition of blastholes (dry or wet) and the initiation systems on generation of flyrock is analysed and the most critical parameters for flyrock control are identified. Based on the analysis of results, suggestions are given to minimise the flyrock hazards at limestone quarries.

1. Introduction

Danger and damage from flyrock in rock blasting has been a serious problem ever since blasting was introduced. Not only have men been killed and injured but also buildings, equipment and materials have been damaged (Lundborg et al., 1975). Flyrock which travels beyond the protected blasting area caused 25% of the blasting accidents in U. S. surface mining (Fletcher and D'Andrea, 1986). An analysis of blasting accidents in Indian mines indicated that more than 40% of fatal and 20% of serious accidents were caused by flyrock (Bhandari, 1997). The major causes of flyrock are inadequate burden, inadequate stemming length, drilling inaccuracy, excessive powder factor, unfavourable geological conditions (open joints, weak seams, cavities), inappropriate delay timing and sequence, inaccuracy of delays, backbreak and loose rock on top of the bench (Fletcher and D'Andrea, 1986; Workman and Calder, 1994; Kopp, 1994; Bhandari, 1997).

The energy spent in creating flyrock during blasting is less than 1% of the total energy transferred to the rock (Berta, 1990), hence the wastage of explosive energy in this form may be insignificant. However, the risk of damage due to flyrock is so high that it merits serious consideration in blast design. Keeping this in view, field investigations were conducted at six limestone quarries to study the flyrock from blasting. This study is restricted to the same type of rock so that the variation in rock mass properties is minimum and the influence of blast design parameters on flyrock distance could be analysed.

2. Field Data

The limestone quarries selected for this study were producing about one million tons per annum. The quarries were developed in two or three benches and deployed similar types of equipment. All the six quarries were operating at more than 500 m distance from the nearest village. Some complaints about blast vibration had been received from the local residents but no complaints were received about flyrock. The quarry had plans to extract limestone in future from the areas close to villages.

The density of limestone varied between 2.5 to 2.68 ton/m^3 and the limestone was medium to hard. Three sets of joints were present and the most prominent one was the bedding plane. Except for thin clay seams occasionally present, other features such as wide open joints, voids and cavities, were absent. Therefore at these quarries, the rock conditions for the generation of flyrock were rated as normal.

Blasthole diameter, burden, stemming length and condition of the holes (watery or dry) were recorded for 47 blasts at six limestone quarries along with the maximum distance travelled by the fragments (Table 1). The actual burdens were recorded for the front row of holes. Drill cuttings were used as stemming material and blasting mats were not used to control flyrock. Subgrade drilling was nil to about 1 m depending on whether horizontal bedding planes at the grade level were present or not. It was difficult to arrange blasts for experimental purpose with higher or lower powder factor. However, in quarry E, powder factor could be varied from 0.30 to 0.98 kg/m^3 against the optimum powder factor of about 0.45 kg/m^3. Other parameters at these quarries were:

Bench height: 6–10 m
Spacing: (1–1.5) Burden
Number of holes per blast: 10–40
Number of rows: 1–3
Number of inert decks per hole: 1–3
Explosives used: ANFO with 15–25% of cap sensitive explosive
Initiation system: Detonating cord downline with
a) detonating cord trunk line and detonating relays
b) electric detonators with or without Sequential Blasting Machine
Maximum acceptable size of fragments: 1.0 m.

3. Analysis of the Data

The observed flyrock distances are used to determine the safe distance for flyrock. The field data are analysed to determine correlation between flyrock distances and the blast design parameters. The existing practices at limestone quarries are compared with the state-of-the-art in blasting technology to identify the areas for improving safety in blasting operations.

Table 1. Base data on flyrock observations at limestone quarries. d: blasthole diameter; B: burden; l_s: stemming length; q: Powder factor; q_0: optimum powder factor (0.45 kg/m^3 for quarry E)

Quarry	d (m)	B (m)	l_s (m)	l_s/B	B/d	l_s/d	Flyrock distance (m)	q (kg/m^3)	q/q_0	Condition of holes
A	0.100	2.7	2.4	0.89	27	24	40	–	–	dry
		2.5	2.4	0.96	25	24	40	–	–	dry
		2.5	2.6	1.04	25	26	60	–	–	dry
		2.4	3.6	1.50	24	36	25	–	–	dry
		2.5	3.2	1.28	25	32	35	–	–	dry
		2.6	3.4	1.30	26	34	40	–	–	dry
B	0.115	2.9	2.5	0.86	25	22	50	–	–	dry
		2.4	2.0	0.83	21	17	150	–	–	watery
		2.5	2.0	0.80	22	17	300	–	–	watery
		2.8	1.9	0.68	24	17	45	–	–	dry
		2.5	2.5	1.00	22	22	40	–	–	dry
		2.5	1.5	0.60	22	13	55	–	–	dry
		2.6	3.1	1.20	23	27	35	–	–	dry
C	0.115	2.8	0.5	0.18	24	4	130	–	–	dry
		3.3	0.5	0.15	29	4	140	–	–	dry
		3.4	0.5	0.15	30	4	160	–	–	dry
		3.0	2.3	0.77	26	20	45	–	–	dry
		3.0	0.4	0.13	26	3	192	–	–	dry
		3.5	0.5	0.14	30	4	150	–	–	dry
		3.0	2.7	0.90	26	23	40	–	–	dry
D	0.150	4.5	2.0	0.44	30	13	100	–	–	watery
		6.0	2.0	0.33	40	13	150	–	–	watery
		5.5	2.0	0.36	37	13	150	–	–	watery
		4.0	2.0	0.50	27	13	250	–	–	watery
		5.0	2.0	0.40	33	13	160			watery
		4.0	2.0	0.50	27	13	100	–	–	watery
		3.5	2.0	0.57	23	13	150	–	–	watery
E	0.115	3.0	1.8	0.60	26	16	120	0.59	1.31	dry
		3.0	2.1	0.70	26	18	120	0.70	1.56	dry
		3.0	2.0	0.67	26	17	50	0.64	1.42	watery
		2.5	1.8	0.72	22	16	120	0.98	2.18	dry
		3.0	2.0	0.67	26	17	50	0.49	1.09	dry
		4.0	1.8	0.45	35	16	50	0.34	0.76	dry
		3.0	2.8	0.94	26	24	50	0.34	0.76	dry
		3.5	2.0	0.57	30	17	50	0.44	0.98	dry
		3.0	2.0	0.67	26	17	150	0.63	1.40	dry
		3.0	2.2	0.73	26	19	40	0.43	0.96	dry
		4.0	2.1	0.52	35	18	300	0.30	0.67	dry
		3.6	3.8	1.05	31	33	100	0.76	1.69	dry
		4.0	2.0	0.50	35	17	150	0.85	1.89	dry
F	0.150	3.5	1.5	0.43	23	10	270	–	–	dry
		3.5	1.5	0.43	23	10	180	–	–	dry
		3.5	1.5	0.43	23	10	130	–	–	dry
		3.5	2.0	0.57	23	13	160	–	–	dry
		3.5	1.5	0.43	23	10	100	–	–	dry
		3.5	2.0	0.57	23	13	50	–	–	dry
		3.5	2.0	0.57	23	13	100	–	–	dry

3.1 Safe Distance for Flyrock

Safe distance is the minimum distance beyond which the throw of fragments does not appreciably affect the surroundings. The Metalliferous Mines Regulations, 1961 prescribes a danger zone of 300 m for surface blasting. As the accidents related to flyrock did occur outside this zone, the Director General of Mines Safety, Dhanbad recommended to increase the radius of the danger zone to 500 m for surface blasting (DGMS, 1982).

Despite some attempts to estimate flyrock distance (Lundborg et al., 1975; Roth, 1979; Chiappetta and Borg, 1983; Workman and Calder, 1994), it is extremely difficult to predict flyrock, both in terms of distance and direction. From Table 1 it is noted that the maximum flyrock distance for all the blasts is 300 m, and this distance plus some safety factor can be used to estimate the safe distance for flyrock. The safe distance of 500 m is therefore reasonable for limestone quarries.

According to the Metalliferous Mines Regulations, 1961, the boundary of the danger zone may be relaxed and blasting permissions may be granted in India on the condition that flying fragments should not go beyond 10 m from the place of blast. Clearly, this clause is too stringent and it may be unnecessary if flyrock can be restricted within one half the distance between the blast and the nearby village through proper blast design and field control. Blasting mats should be used when flyrock cannot be controlled to this extent by the blast design itself.

3.2 The Influence of Burden

As the blasthole diameters (d) used at these quarries are different, the burden (B) is expressed as multiples of blasthole diameter and flyrock distances are plotted against the burden to hole diameter (B/d) ratio (Fig. 1). It should not be interpreted that burden has no influence on flyrock. From single hole tests (Bilgin,

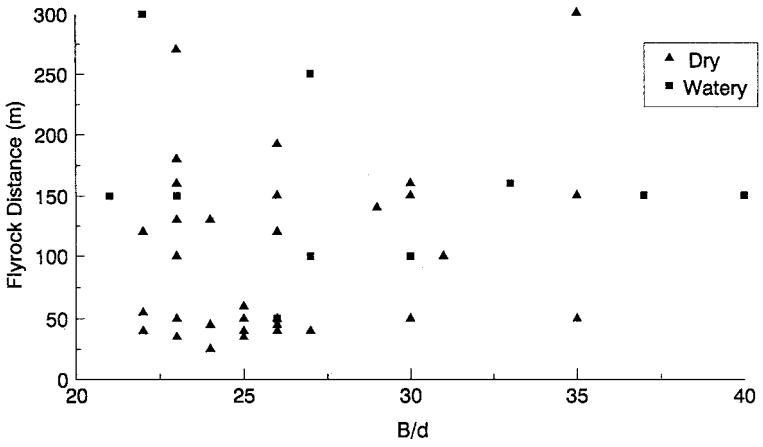

Fig. 1. Influence of burden (B) to blasthole diameter (d) ratio on flyrock

1991), it is known that the flyrock decreases as the burden increases. In the present study, the variation of burden distance is not large enough to observe the behavior of flyrock as in the case of single hole tests. Moreover, the burden of 20–40 times the blasthole diameter is within the accepted range (Bhandari, 1997).

It is possible to obtain crater effects from the front row of holes if burden is inadequate. This may be due to incorrect design, drilling errors and geological weakness. Proper care and precautions are to be taken while marking and drilling the holes, particularly for the front row of holes.

3.3 The Influence of Stemming Length

The stemming length (l_s) is also expressed as multiples of blasthole diameter (d) and plot of flyrock distance against stemming length to hole diameter (l_s/d) ratio is shown in Fig. 2. The maximum flyrock distance decreases with an increase in stemming length and does not exceed 100 m when $l_s/d \geq 20$. The decreasing trend of flyrock distance with increasing stemming length is obvious from the role of confinement in controlling premature venting of high pressure gases.

Field experiments carried out in Sweden using high speed photography indicated that the throw length increased with increasing stemming length. The maximum throw was achieved for $l_s/d \approx 10$; and then it decreased again. Persson et al. (1994) has provided an explanation for this phenomenon. When the stemming length is short, shock wave component of the explosive energy is sufficient to fragment the rock at the collar. If the rock is finely fragemented, the small fragments will not be thrown very far because they have a very low mass and are stopped effectively by the air drag. If the stemming length is long, large pieces of rock will form. They have large mass and, for the same impulse, their velocity and throw distance will be consequently short. Between these two extremes, a maximum throw distance may be expected.

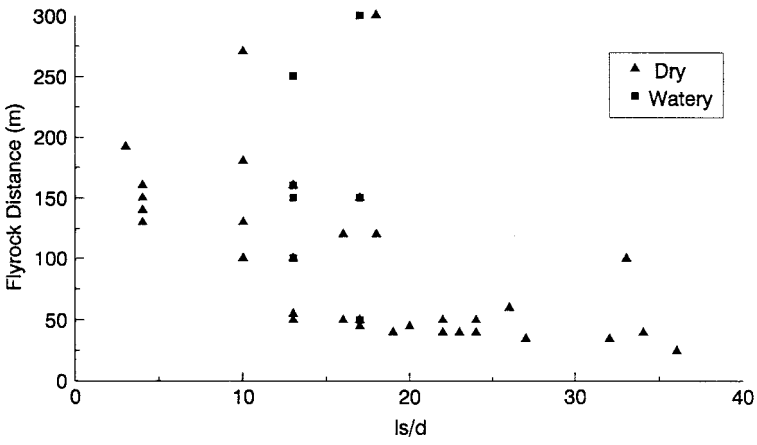

Fig. 2. Influence of stemming length (l_s) to blasthole diameter (d) ratio on flyrock

When this explanation is applied to the present data (Fig. 2), the trend remains the same except for two points with the maximum throw of 300 m. These two data may be due to some other factors as l_s/d ratios are close to 20.

It is noted that stemming is the most neglected blast design parameters at limestone quarries. Some consideration is given to the stemming length but no consideration is given to the stemming material and particle size of the material. Hence, there is scope for reducing flyrock at these quarries by ensuring $l_s/d \geq 20$ and by using suitable stemming material, such as angular gravel (Konya and Walter, 1990).

3.4 The Influence of Stemming Length to Burden Ratio

Taking flyrock distance as a dependent variable, stemming length to burden (l_s/B) ratio (a dimensionless parameter) as independent variable, three types of regression analysis (linear, exponential and power curve) were carried out. Four values of flyrock distance (>200 m) that deviated very much from the rest of the data were not included in the regression analysis.

The correlation between flyrock distance and l_s/B ratio is significant for the combined data from all quarries. The correlation is negative, showing a decreasing trend of flyrock distance with increasing l_s/B ratio as shown in Fig. 3. These relationships are valid only for l_s/B ratio of 0.13 to 1.5. They should not be used to calculate the flyrock distance if the blastholes are accidentally charged up to the collar. These equations may be used to know the trend but should not be used to calculate the safe distance for flyrock.

The exponential curve fits better than the linear or power curve based purely on r^2 value. The linear equation intersecting X-axis at a steep angle is not accepted because flyrock does not decrease significantly for $l_s/B \geq 1.2$. Both the exponential and power curves show that flyrock increases sharply with the decreasing l_s/B ratio and decreases very marginally when the ratio becomes 1 or greater. Since the confinement to a blast is provided by burden and stemming, it is logical that the ratio should be 1.0. With large hole diameter, long stemming columns would cause unsatisfactory fragmentation if thickly bedded, hard limestone occurs in the stemming zone. This is the reason why shorter stemming length is used at limestone quarries. However, $l_s/B = 0.7$ is a must with conventional stemming. If fragmentation problem exists, satellite holes (short holes) or pocket charges may be considered as practised in some other limestone quarries in India.

Flyrock, air blast and fragmentation can all be controlled by using blasthole plugs and air decking. By incorporating blasthole plugs (Worsey, 1990), substantial reductions in stemming ejection velocity or ejection elimination have been achieved, while reducing the stemming length up to 35% over conventional practices. Air decking (Mead et al., 1993) increases the level of fragmentation in the stemming zone without increasing flyrock or stemming ejection.

In Fig. 3, the maximum distances to which fragments were thrown away from the blast are marked differently for watery and dry holes. Seven out of eight points from watery holes are above the regressed line of the power curve (Fig. 3c),

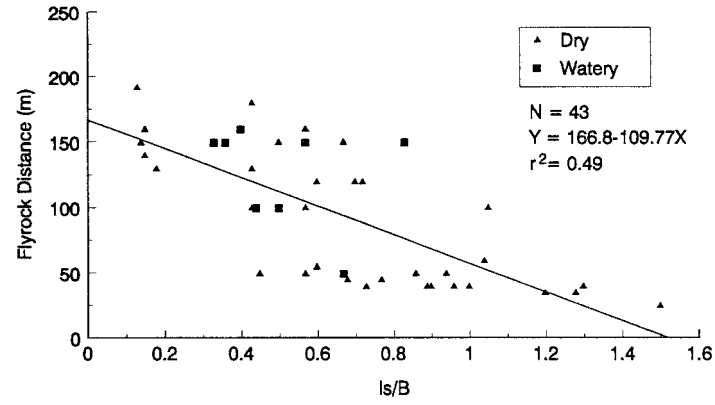

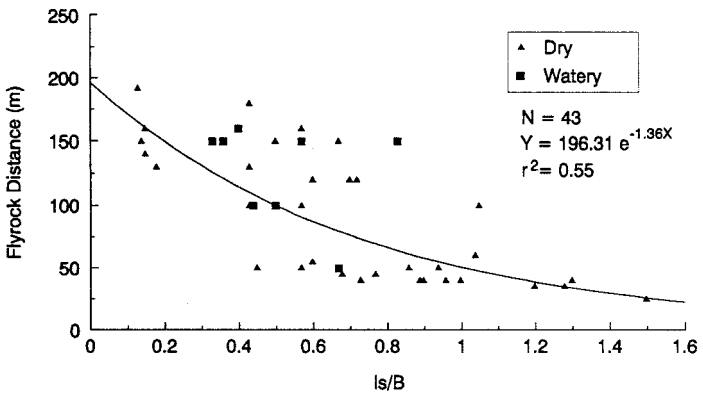

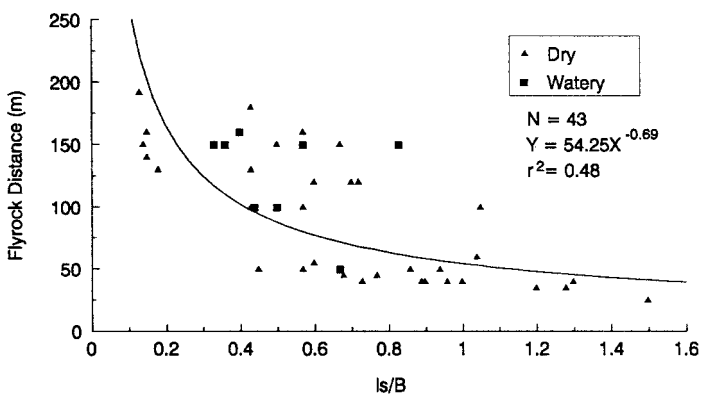

Fig. 3. Trend of flyrock with stemming length (l_s) to burden (B) ratio. Y = flyrock distance; $X = l_s/B$; N Number of observations; r^2 index of determination

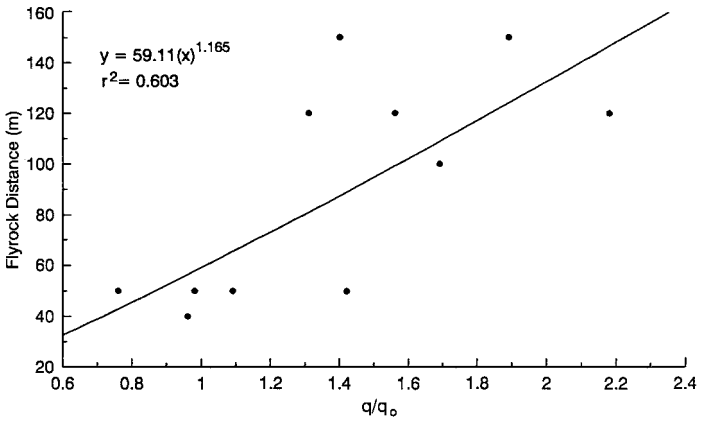

Fig. 4. Trend of flyrock with powder factor. y = flyrock distance; $x = q/q_0$ where q powder factor used and q_0 optimum powder factor; r^2 index of determination

confirming that watery holes favour the occurrence of flyrock. The water in the blasthole exerts significant influence when it rises up to the stemming column. The drill cuttings used as stemming material form slurries which cannot provide adequate confinement to the borehole pressure. The gaseous energy is vented into the atmosphere causing flyrock. The effect of water on flyrock may be reduced by dewatering blastholes or by using suitable stemming material.

3.5 The Influence of Powder Factor

The powder factor data for quarry E (Table 1) are expressed as the ratio of q/q_0, where q is the powder factor used in the blast and q_0 is the optimum powder factor and the relationship between flyrock and q/q_0 is shown in Fig. 4. One reading with $q/q_0 = 0.67$ and flyrock distance equal to 300 m is not included in the graph. When $q/q_0 = 2$, flyrock increases by 2.24 times as compared to $q/q_0 = 1$. It can be seen from the figure that flyrock is within 60 m when $q/q_0 \leq 1.15$. Previous study (Lundborg et al., 1975) also shows that flyrock can be avoided if the powder factor is smaller than a critical value. However, it is not recommended to reduce the powder factor significantly because it will adversely affect the fragmentation and displacement. An optimum powder factor can satisfy both economic and environmental considerations in blast design. Excess powder factor is not used at limestone quarries and unless charge concentration becomes high due to undetected geological structures, excessive explosive consumption is not the cause of flyrock at these quarries.

3.6 The Influence of Blasthole Diameter

When a blasthole diameter is increased, the loading density of fully coupled charges increases by the square of the ratio of the diameters. This means that,

when changing from a 100 mm diameter to 200 mm diameter, the loading density increases four times. This increase in explosive energy under unfavourable geological conditions (presence of voids, mud seams, open joints) with inadequate burden or poor stemming may produce excessive flyrock.

Using a semi-empirical method, Lundborg et al. (1975) has derived the following equation to estimate maximum flyrock distance:

$$L_{\max} = 260\, d^{2/3},$$

where

$L_{\max}$ = maximum flyrock distance (m)

d = hole diameter (inch).

This equation shows that maximum flyrock distance increases 1.58 times when hole diameter is increased from 100 mm to 200 mm. It is established that the risk of flyrock increases with large hole diameter. While blasting close to inhabitants, smaller diameters are recommended to minimise the flyrock and ground vibration hazards.

The effect of blasthole diameter could not be studied over a wide range as the quarries used hole diameters between 100 and 150 mm. As expected, flyrock distance is least for 100 mm diameter, but it is greater for 115 mm than for 150 mm. This may be due to difference in the size of the fragments. It is felt that the size of fragments should also be recorded as the maximum throw distance is the function of hole diameter and diameter of the fragments (Lundborg et al., 1975).

3.7 The Influence of Initiation Systems

Significant progress has been made during the last two decades in the areas of blasthole initiation and development of initiating devices. The influences of delay timing and sequence on generation of flyrock are known (Konya and Walter, 1990; Bhandari, 1997), but the degree to which flyrock can be controlled is also influenced by the selected initiation system. For the various initiation methods commonly used at limestone quarries, the probability of occurrence of flyrock is illustrated in Fig. 5 for a case of 24 holes drilled in three rows.

If the individual holes are connected with short delay electric detonators (Fig. 5a), there is a probability of overlap due to scattering of delay periods. If any of the succeeding detonators in the second or third row fires earlier than the preceding detonator, it would cause cratering and generation of flyrock from top of the bench. The problem still exists if the group of holes are connected with detonating cord and initiated by short delay electric detonators (Fig. 5b).

If the holes are initiated with detonating cord relay system (Fig. 5c), the initiation proceeds sequentially and the problem of flyrock due to overlap does not arise. However, there is limited scope for optimising the delay intervals as the detonating relays have fixed intervals.

A group of holes can be connected with detonating cord, which in turn is connected to instantaneous electric detonators. The delays are provided with cir-

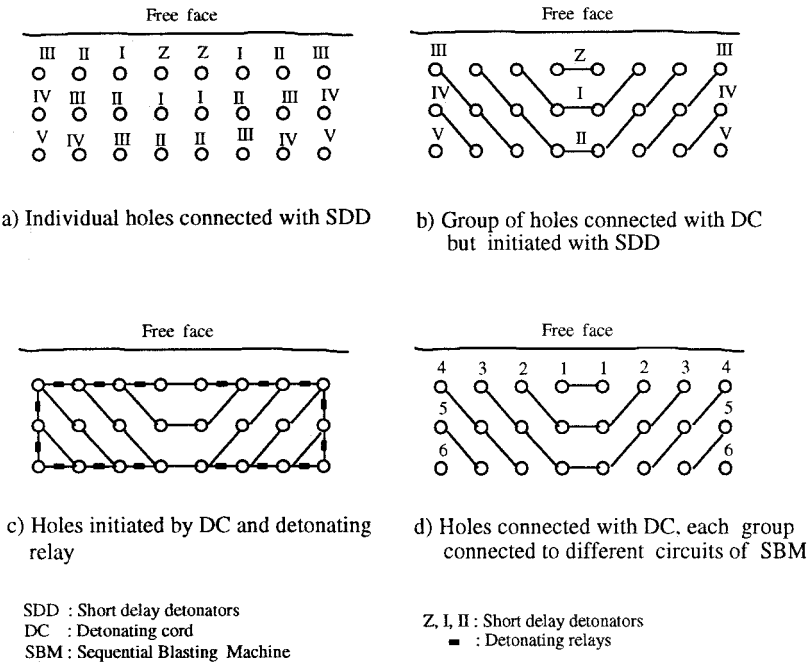

Fig. 5. Influence of initiation systems on generation of flyrock

cuit delays of the Sequential Blasting Machine (Fig. 5d). In this case, the delays are accurate and the delay intervals can be optimised to control flyrock.

The detonation of a 10 gm/m detonating cord downline, being used in limestone quarries, can laterally compress the stemming material (drill cuttings) so as to create a gas chimney through which gases can escape into the atmosphere. The detonating cord downline system should be replaced by the shock tube initiation system or low energy detonating cord. Besides flyrock control, there are several advantages of these initiation systems (Konya and Walter, 1990; Bhandari, 1997).

4. Conclusions

The maximum flyrock distance observed at limestone quarries is 300 m and the safe distance of 500 m is reasonable. Unless the existing practices at limestone quarries are improved, it may be difficult to extract limestone deposits which are located close to dwellings.

This study aimed at determining blast design parameters responsible for flyrock at limestone quarries and identifying the areas for immediate attention. Though blasthole diameter, burden and powder factor are common causes of flyrock, poor stemming performance is the major cause of flyrock at these limestone quarries. It is established that the stemming length should not be less than 20 times the blasthole diameter and 0.7 times the burden. The risk of flyrock is

greater when the stemming is saturated with water. It is noted that the research findings for stemming efficiency (suitable stemming material, blasthole plugs and air decking) have not been put into practice at these quarries. Blasthole initiation appears to be the second major cause of flyrock. Flyrock can be controlled by introducing better initiation techniques. All these factors are related to blast design and thus the flyrock can be significantly controlled by improving the existing blasting practices at limestone quarries.

References

Berta, G. (1990): Explosives: an engineering tool. Italesplosivi, Milano.

Bhandari, S. (1997): Engineering rock blasting operations. A. A. Balkema, Rotterdam.

Bilgin, H. A. (1991): Single hole test blasting at an open pit mine in full scale: a case study. Int. J. Surf. Min. Reclam. 5(4), 191–194.

Chiappetta, R. F., Borg, D. G (1983): Increasing productivity through field control and high-speed photography. Proc., 1st Int. Symp. on Rock Fragmentation by Blasting, Lulea, Sweden, 301–331.

DGMS (1982): Directorate General of Mines Safety. Technical Circular No. 8. Dhanbad, India.

Fletcher, L. R., D'Andrea, D. V. (1986): Control of flyrock in blasting. Proc., 12th Conf. on Explosives and Blasting Technique, Atlanta, Georgia, 167–177.

Konya, C. J., Walter, E. J. (1990): Surface blast design. Prentice-Hall, Englewood-Cliffs.

Kopp, J. W. (1994): Observation of flyrock at several mines and quarries. Proc., 20th Conf. on Explosives and Blasting Technique, Austin, Texas, 75–81.

Lundborg, N., Persson, A., Ladegaard-Pedersen, A., Holmberg, R. (1975): Keeping the lid on flyrock in open-pit blasting. Engng. Min. J. 176, May, 95–100.

Mead, D. J., Moxon, N. T., Dannel, R. E., Richardson, S. B. (1993): The use of air-decks in production blasting. Proc., 4th Int. Symp. Rock Fragmentation by Blasting, Vienna, Austria, 437–443.

Persson, P. A., Holmberg, R., Lee, J. (1994): Rock blasting and explosives engineering. CRC, Atlanta.

Roth, J. (1979): A model of the determination of flyrock range as function of shot conditions. A report for the U. S. Bureau of Mines by Management Services Association, Los Altos, California, NTIS, PB81-222358.

Workman, J. L., Calder, P. N. (1994): Flyrock prediction and control in surface mine blasting. Proc., 20th Conf. on Explosives and Blasting Technique, Austin, Texas, 59–74.

Worsey, P. (1990): Stemming ejection comparison of conventional stemming and stemming incorporating blast control plugs for increasing explosion energy use. Proc., 3rd Int. Symp. on Rock Fragmentation by Blasting, Brisbane, 361–367.

Author's address: Dr. G. R. Adhikari, National Institute of Rock Mechanics, Champion Reefs PO, Kolar Gold Fields 563 117, Karnataka, India.

Rock Mech. Rock Engng. (2006) 39 (2), 159–168
DOI 10.1007/s00603-005-0044-9

Rock Mechanics and Rock Engineering
Printed in Austria

Technical Note

Comparison of Fragmentation Measurements by Photographic and Image Analysis Techniques

By

J. Sudhakar, G. R. Adhikari, and **R. N. Gupta**

National Institute of Rock Mechanics, Kolar Gold Fields, India

Received June 1, 2004; accepted December 20, 2004
Published online May 2, 2005

Keywords: Fragmentation, image analysis, photographic analysis, fragment size distribution.

1. Introduction

The primary objective of rock blasting is fragmentation but it is extremely difficult to assess the degree of fragmentation. Sieving/screening is a direct and accurate method of evaluation of size distribution of particles or fragmentation. However, for production blasting, this method is costly, time-consuming and inconvenient. Therefore, indirect methods, such as photographic methods have been in use in blasting research (Rholl, 1987; Nie and Rustan, 1987; MacLachlan, 1989). With the advances in technology, digital images processing and analysis systems are becoming increasingly popular in fragmentation measurement due to their advantages over photographic methods.

Research work has been carried out all over the world in developing image analysis systems. Several countries/organisations have developed their own image analysis systems. Some of these systems include IPACS (Dahlhielm, 1996), TUCIPS (Havermann and Vogt, 1996), FRAGSCAN (Schleifer and Tessier, 1996), CIAS (Downs and Kettunen, 1996), GoldSize (Kleine and Cameron, 1996), WipFrag (Maerz et al., 1996), SPLIT (Kemeny, 1994), PowerSieve (Chung and Noy, 1996) and Fragalyst (Raina et al., 2002). Though these systems claim that they are suitable for rock fragmentation analysis, limited field experiments have been conducted so far to check the validity of the results. Liu and Tran (1996) revealed that the results of fragmentation determined by three different image analysis systems were not the same. Among the available image analysis systems, WipFrag and Fragalyst are used

in India. It is not known whether the results of fragmentation analysis of the same blast by both the systems are comparable. With this in view, size distributions of 10 photographs of a dragline blast in sandstone rock were determined by WipFrag, Fragalyst and photographic (manual) methods and the same were compared.

2. Techniques Used for Fragmentation Analysis

Photographs of a blasted muck of a dragline bench in sandstone were taken at a regular interval of half-an-hour. Analyses of ten photographs were done by using three methods, namely manual, WipFrag and Fragalyst. The last two methods are based on image analysis.

2.1 Photographic/Manual Analysis

Delineating of fragments on each of the photographs was carried out manually. For this, photographs of $0.15\,\text{m} \times 0.10\,\text{m}$ size were printed. Each photograph was placed under the transparent paper by fixing it firmly with the help of pins. All the fragments were delineated on the transparent paper. Delineation was started with large fragments because they are having more effect on the results. It was tried to detect and delineate fragments as small as possible. The scale placed in the middle of the muck pile was used to convert the measured distance on the photograph to actual distance. The manual analysis of each photograph took about one to two hours.

Then, a xerox copy of the traced paper was placed on a graph paper. The area of the reference scale on graph paper was noted down and then a scale factor (actual area of scale/graph area of scale) was determined. For every identifiable fragment, the area covered by the fragment was measured by counting the number of small blocks on the graph paper covered by that fragment was multiplied with the scale factor. For converting the area into volume, the third dimension was determined using the method of equivalent circle of area (Maerz et al., 1987; MacLachlan et al., 1989). The parameters are calculated as follows:

$$\text{Equivalent diameter} = \text{SQRT}\ (4 * \text{Area}/\Pi),\ \text{m}$$

$$\text{Spherical volume} = \text{Area} \times \text{Equivalent diameter},\ \text{m}^3$$

$$\text{Weight of the fragment} = \text{Spherical volume} \times \text{density of the rock, kg}$$

2.2 Image Analysis Using Fragalyst and WipFrag

Fragalyst (Raina et al., 2002) is an image analysis system developed by CMRI Regional Centre, Nagpur (India) and Wavelet Group of Pune (India). This system consists of capturing video photographs of the muck pile, down loading the photographs to the computer, or capturing the photos of muck pile from field by digital camera/ordinary camera then converting the images to grey scale, image enhancement, calibration and blob (grain) analysis. With the aid of menu-driven software, it is possible to determine the area, size and shape of the fragments in a muck pile/grain aggregates on the basis of grey scale difference. The 2-D information available from software can further be processed for stereological analysis for 3-D information.

Table 1. Comparison of automatic and manual netting of fragments by WipFrag

Photo no.	Mean fragment size, m		Uniformity index		Characteristic size, m		No. of fragments		Maximum fragment size, m	
	A	M	A	M	A	M	A	M	A	M
1	0.53	0.45	1.11	1.21	0.90	0.56	761	418	2.28	1.29
2	0.72	0.57	1.45	0.95	1.01	0.69	576	350	2.15	1.67
3	0.31	0.41	1.47	0.60	0.44	0.60	1368	459	2.16	2.78
4	0.45	0.83	1.33	0.77	0.57	1.12	868	321	1.29	3.59
5	0.44	0.37	1.31	1.05	0.67	0.45	974	354	2.16	1.00
6	0.56	0.49	1.23	1.02	0.88	0.69	1001	294	2.78	2.15
7	0.27	0.46	1.16	1.08	0.42	0.55	484	269	1.67	1.29
8	0.54	0.49	1.38	0.89	0.78	0.66	777	407	1.80	2.78
9	0.40	0.43	1.48	1.24	0.56	0.53	1000	262	2.46	1.00
10	0.51	0.44	1.16	1.16	0.83	0.58	808	341	2.39	1.29

Note: A = automatic, M = manual.

WipFrag is an image analysis system for sizing materials such as blasted or crushed rock. It was developed by Wipware, Inc, Canada (Maerz et al., 1996). It accepts images from a variety of sources such as camcorders, fixed cameras, photographs, or digital files. It uses automatic algorithms to identify individual blocks, and create an outline 'net'. WipFrag measures the 2-D net and reconstructs a 3-D distribution using principles of geometric probability. The system allows various types of output according to individual requirements, including cumulative size distribution graphs and percentage passing at different sieve sizes. Both WipFrag and Fragalyst allow combining results from several images called merging.

Fragmentation characteristics such as mean fragment size, uniformity index and characteristic size were calculated using automatic and manual netting facilities of ten photographs for WipFrag and the results are compared in Table 1.

Automatic netting produced larger mean fragment size in some cases due to the failure of software to recognize boundaries between clusters of fine particles, which were counted as single fragment, said to be ''fusion''. In other cases, automatic netting produced lower mean fragment size as some large fragments were broken into many smaller fragments, said to be ''disintegration''. Disintegration plays a crucial role in results because it affects large fragments and large volume. Automatic netting also produced high values of uniformity index in almost all the cases due to false identification of fines as fragments and fission of some coarser fragments into smaller. Delineation of fragments in each photograph was done manually after auto netting, generated by the image analysis systems.

3. Comparison of Individual Results

The fragment size distribution curves for all 10 photographs (samples) determined by all the three methods are plotted in Fig. 1. The mean fragment size, uniformity index and characteristic size for all samples are also given in Table 2. The mean fragment size determined by one method differs from the other as much as twice and is not

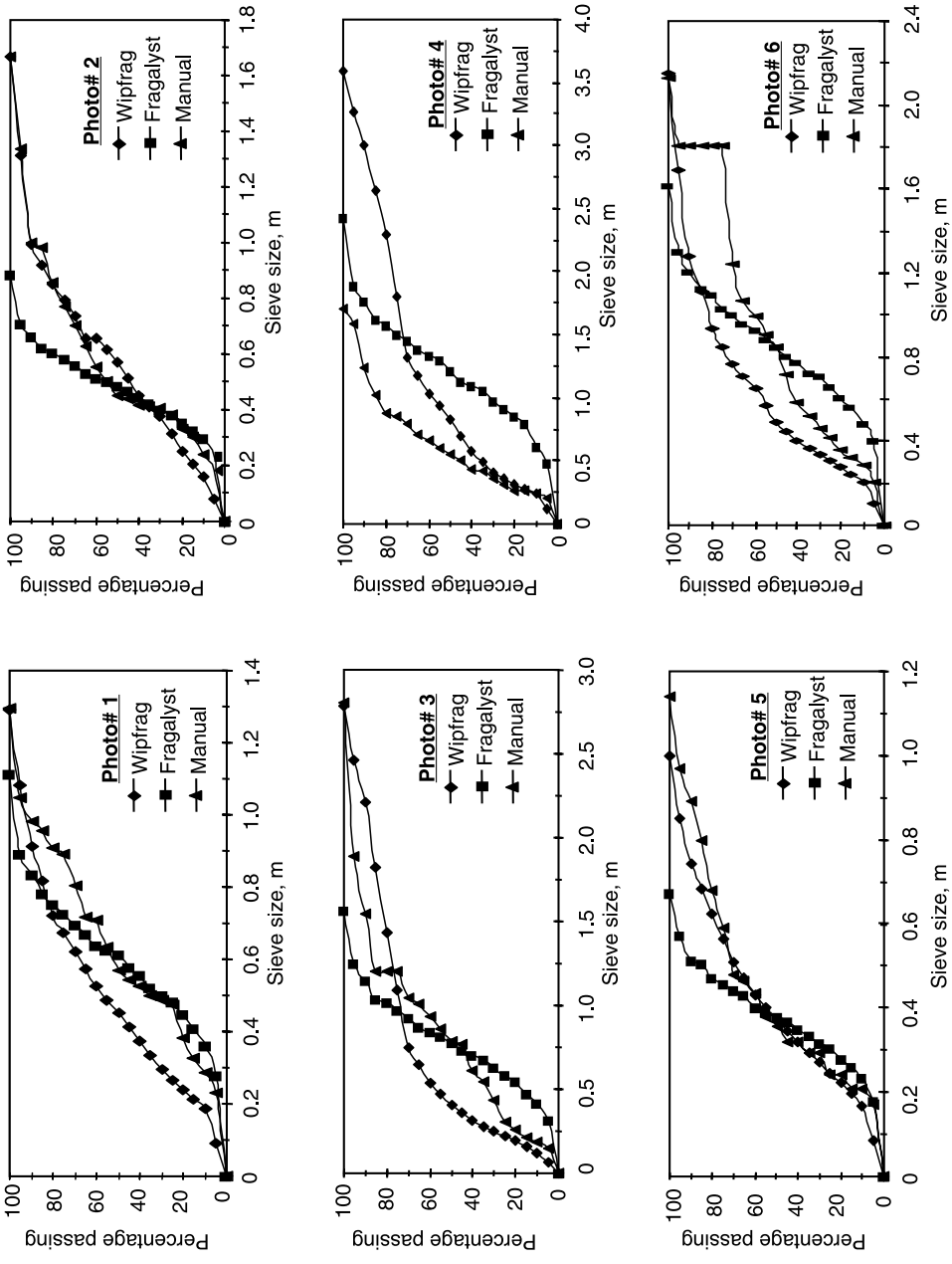

Fig. 1a. Fragment size distribution of individual samples (photographs 1 to 6) using WipFrag, Fragalyst and Manual method

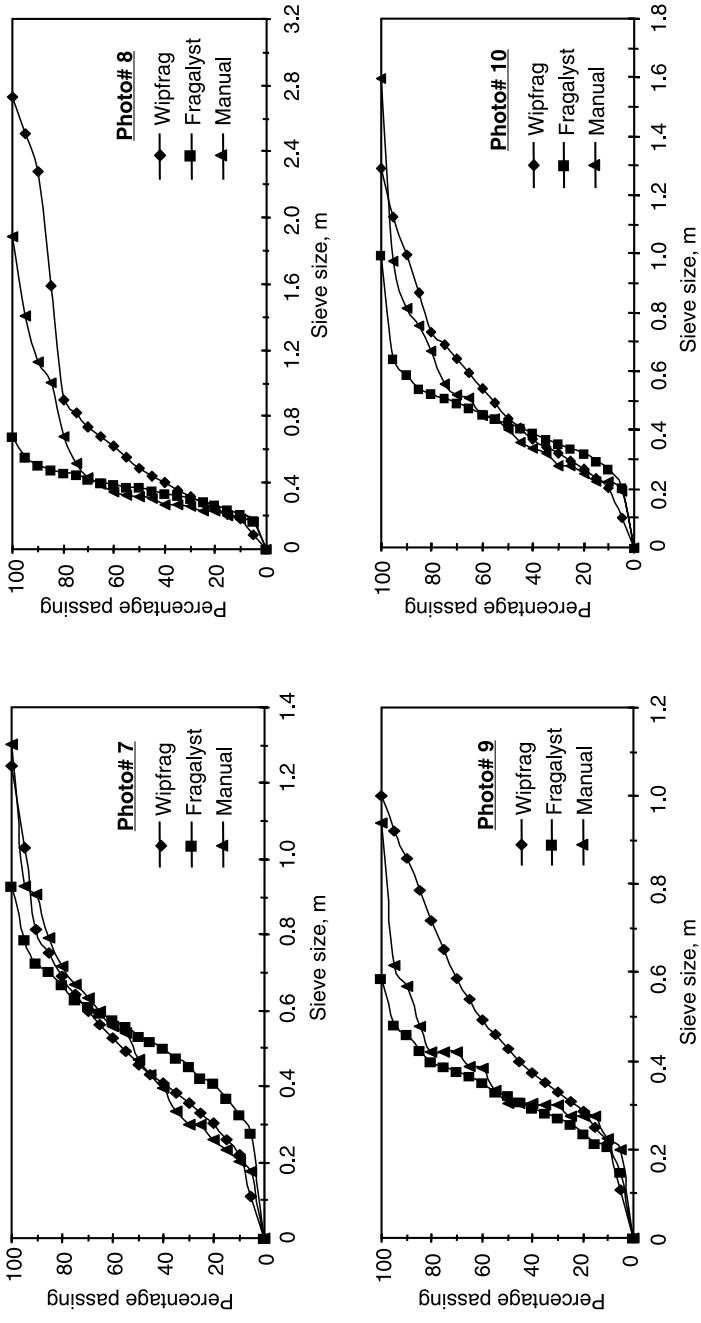

Fig. 1b. Fragment size distribution of individual samples (photographs 7 to 10) using WipFrag, Fragalyst and Manual method

Table 2. Fragmentation characteristics of 10 samples determined by Fragalyst, WipFrag and manual method

Photo no.	Mean fragment size, m			Uniformity index		Characteristic size, m		
	F	W	M	F	W	F	W	M
1	0.59	0.45	0.57	3.66	1.21	0.66	0.56	0.72
2	0.48	0.57	0.45	3.74	0.95	0.53	0.69	0.57
3	0.76	0.41	0.79	3.19	0.60	0.85	0.60	0.93
4	1.19	0.83	0.55	3.22	0.77	1.33	1.12	0.69
5	0.37	0.37	0.36	3.92	1.05	0.41	0.45	0.45
6	0.84	0.49	0.85	3.51	1.02	0.93	0.69	1.07
7	0.53	0.46	0.47	4.02	1.08	0.58	0.55	0.59
8	0.36	0.49	0.31	3.64	0.89	0.40	0.66	0.39
9	0.32	0.43	0.31	3.68	1.24	0.35	0.53	0.38
10	0.42	0.44	0.40	3.94	1.16	0.46	0.58	0.51

Note: F = Fragalyst, W = WipFrag, M = Manual.

consistently higher or lower for a particular method. Fragalyst indicates lower percentage of fines than the other two methods. At 100% passing, WipFrag and manual methods show larger fragment sizes compared to Fragalyst. The size distribution curves for manual analysis are not as smooth as for other methods.

The uniformity index estimated by Fragalyst is always greater than 3, which according to Cunningham (1983) corresponds to very uniform distribution, not common to blasted muck pile. The uniformity index obtained from WipFrag on the contrary is less than 1.5, which is normally expected in practical mining conditions. The maximum size of fragments at 100% passing computed by Fragalyst is much smaller than by other two methods. It appears that Fragalyst has underestimated the range of fragmentation, leading to higher uniformity index.

The difference in the fragmentation results could be due to different capability of the methods in detecting edges of fragments, resolution of fines and areas to volume transformations.

4. Comparison of the Merged Results

As the fragmentation within a blast was not uniform, several images were merged to estimate the representative size distribution of the blast. Though it was not possible to cover the entire muck pile of a dragline blast with these 10 photographs, yet the merged results were obtained in this study. The merging facility was available with WipFrag and Fragalyst. In case of the manual method, all the individual results of 10 photographs were combined and mass passing percentage at various sieve sizes were found. The merged results of all of these methods are shown in Fig. 2.

Manual and WipFrag analyses produced similar distributions but Fragalyst produced coarser results. The difference in the mean fragment size was 2.6% between WipFrag and manual analysis whereas it was 30.3% between Fragalyst and WipFrag. Possibly, Fragalyst underestimated the percentage of fines, resulting in coarser fragmentation.

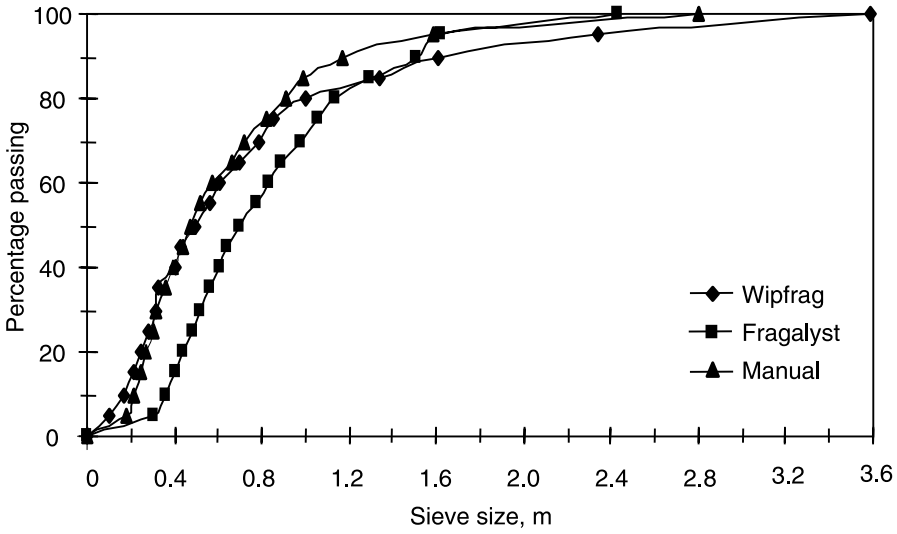

Fig. 2. Merged results of WipFrag, Fragalyst and Manual analysis

5. Correction of Fines Using Rosin-Rammler Equation

A major part of the explosive energy in rock blasting is consumed in creation of a significant amount of fines. The comparison of results of three image analysis systems, FRAGSCAN, WipFrag and SPLIT with sieve analysis results showed that the fines were underestimated by all the three systems because fines were hidden between the coarser fragments or they are simply too small to be resolved. As a result, image analysis tends to overestimate the mean size of the distribution and underestimates the variability of the distribution.

In order to estimate the fines and boulders, the Rosin-Rammler equation (Cunningham, 1983) has been applied. This equation has been extensively used in comminution and blasting and is given by:

$$R = e - (X/Xc)^n, \tag{1}$$

where

R = Factions retained on the screen,
X = Sieve size, m
Xc = Characteristic size, m
n = Uniformity index

Table 3. Adjusted characteristic size and uniformity index

	Measured from Fig. 2		Calculated from Eqs. (2) and (3)	
	k_{50}	k_{80}	Xc	n
Manual	0.49	0.99	0.67	1.18
WipFrag	0.70	1.13	0.86	1.76
Fragalyst	0.48	0.91	0.63	1.31

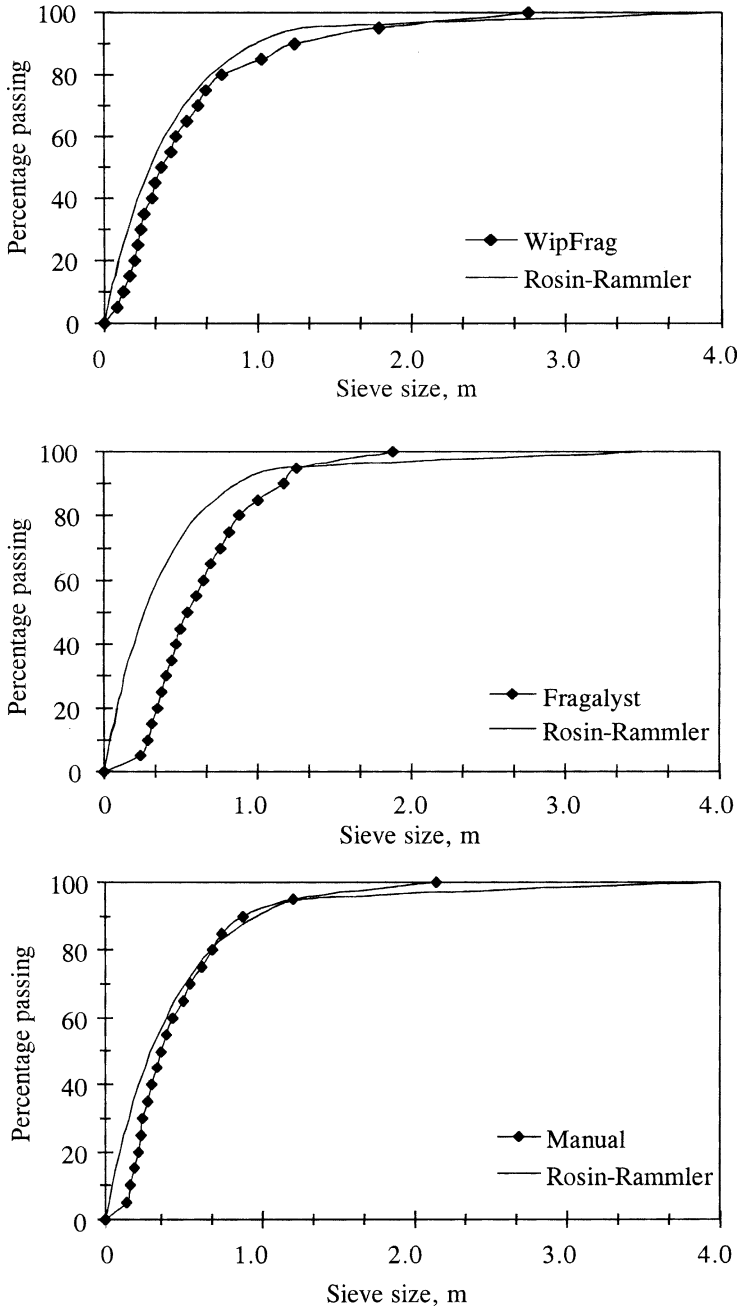

Fig. 3. Comparison of measured fragmentation with the adjusted Rosin-Rammler curve for WipFrag, Fragalyst and Manual analysis

This equation requires two parameters *Xc* and *n* to calculate the entire range of size distribution. These parameters could be calculated from the KUZRAM Model (Cunningham, 1983). This was not done because Chung and Katsabanis (2000) noted serious discrepancies between actual and computed uniformity indices. To overcome these discrepancies, the following empirical relations were suggested for calculation of *Xc* and *n*.

$$Xc = e^{0.565 \times \ln k_{50} + 0.435 \times \ln k_{80}}, \tag{2}$$

$$n = 0.842/(\ln k_{80} - \ln k_{50}), \tag{3}$$

where,

k_{50} = Sieve size at 50% material passing, m
k_{80} = Sieve size at 80% material passing, m
Xc and *n* as defined in Eq. (1).

The k_{50} and k_{80} values were taken from the merged results and the values of Xn and n were calculated (Table 3). After converting the fractions retained into percentage passing, the Rosin-Rammler curves corresponding to the measured distributions are shown in Fig. 3. The deviation of the sieve size at k_{50} from the adjusted Rosin-Rammler curve is about 26% for WipFrag, 107% for Fragalyst and 24% for manual analysis. This indicates that Fragalyst is the least accurate with respect to fines content and needs further improvement.

6. Conclusions

Fragmentation measurements of ten samples were carried out using a manual (photographic) and two image analysis systems. The photographic method was slow and the automatic netting facilities available with the image processing and analysis systems were not sufficient and required manual editing to improve the fidelity of the netting. The fragmentation results from three methods did not agree for individual samples. When merged, WipFrag and manual analysis produced nearly identical distributions but the Fragalyst results deviated significantly. The merged results were uniform and hence, the merging of several individual images for the same blast should be done to get the distribution of the entire muck pile. The Rosin-Rammler curves fitted to the merged distributions showed close agreement between the two in case of manual and WipFrag analyses. The curve deviated remarkably in case of Fragalyst, which appears to have underestimated the fines. Further improvement should be done to overcome the present limitations to make image analysis a practical tool for rock blasting.

References

Chung, S. H., Katsabanis, P. D. (2000): Fragmentation prediction using improved engineering formula. FRAGABLAST – Int. J. Blast. Fragment. 4, 198–207.

Chung, S. H., Noy, M. J. (1996): Experience in fragmentation control. In: Franklin, J. A., Katsabanis, P. D. (eds.), Measurement of blast fragmentation. Balkema, Rotterdam, 247–252.

Cunningham, C. V. B. (1983): The Kuz-Ram model for prediction of fragmentation for blasting. In: Holmberg, R., Rustan, A. P. (eds.), 1st International Symposium on Rock Fragmentation by Blasting, Lulea, Sweden, 47–52.

Dahlhielm, S. (1996): Industrial applications of image analysis – The IPACS system. In: Franklin, J. A., Katsabanis, P. D. (eds.), Measurement of blast fragmentation. Balkema, Rotterdam, 59–65.

Downs, D. C., Kettunen, B. E. (1996): On-line fragmentation measurement utilizing the CIAS system. In: Franklin, J. A., Katsabanis, P. D. (eds.), Measurement of blast fragmentation. Balkema, Rotterdam, 79–82.

Havermann, T., Vogt, W. (1996): TUCIPS – A system for the estimation of fragmentation after production blasts. In: Franklin, J. A., Katsabanis, P. D. (eds.), Measurement of blast fragmentation. Balkema, Rotterdam, 67–71.

Kemeny, J. M. (1994): Practical technique for determining the size distribution of blasted benches, waste dump and heap leach sites. Min. Engng. 1994, 1281–1284.

Kleine, T. H., Cameron, A. R. (1996): Blast fragmentation measurement using GoldSize. In: Franklin, J. A., Katsabanis, P. D. (eds.), Measurement of blast fragmentation. Balkema, Rotterdam, 83–89.

Liu, Q., Tran, H. (1996): Comparing systems – validation of FragScan, WipFrag and Split. In: Franklin, J. A., Katsabanis, P. D. (eds.), Measurement of blast fragmentation. Balkema, Rotterdam, 151–156.

Maclachlan, R. R., Singh, A. (1989): Photographic determination of oversize particles of heaps of blasted rock. J. South Afr. Inst. Min. Metallurgy 89, 147–152.

Maerz, N. H., Franklin, J. A., Ruthenburg, L., Coursen, D. L. (1987): Measurement of rock fragmentation by digital photoanalysis. 6th International Congress. On Rock Mechanics, Montreal, Canada 1, 687–692.

Maerz, N. H., Palangio, T. C., Franklin, J. A. (1996): WipFrag image based granulometry system. In: Franklin, J. A., Katsabanis, P. D. (eds.), Measurement of blast fragmentation. Balkema, Rotterdam, 91–98.

Nie, S.-L., Rustan, A. (1987): Techniques and procedures in analysing fragmentation after blasting by photographic method. In: Proc., 2nd International Conference on Rock Fragmentation by Blasting, Keystone, Colorado, 102–113.

Raina, A. K., Choudhury, P. B., Ramulu, M., Chrakraborty, A. K., Dudhankar, A. S. (2002): Fragalyst – an indigenous digital image analysis system for grain size measurement in mines. J. Geol. Soc. India 59, 561–569.

Rholl, S. A., Grannes, S. G., Stagg, M. S. (1987): Photographic assessment of the fragmentation distribution of rock quarry muck piles. In: 4th International Symposium on Rock Fragmentation by Blasting, Vienna, Austria, 501–506.

Schleifer, J., Tessier, B. (1996): FRAGSCAN: A tool to measure fragmentation of blasted rock. In: Franklin, J. A., Katsabanis, P. D. (eds.), Measurement of blast fragmentation. Balkema, Rotterdam, 73–78.

Authors' address: Dr. G. R. Adhikari, Head, Excavation Engineering, National Institute of Rock Mechanics, Kolar Gold Fields 563 117, India; e-mail: gradhikari@rediffmail.com

Mining Science and Technology, 8 (1989) 297–300
Elsevier Science Publishers B.V., Amsterdam – Printed in The Netherlands

INFLUENCE OF ROCK PROPERTIES ON BLAST-INDUCED VIBRATION

G.R. Adhikari and M.M. Singh

Central Mining Research Station, Dhanbad 826 001 (India)

R.N. Gupta

Department of Mining Engineering, Indian School of Mines, Dhanbad 826 004 (India)

(Received August 12, 1988; revised and accepted December 23, 1988)

ABSTRACT

Ground vibrations induced by blasting have been recorded at various sites. Propagation equations relating peak particle velocity, charge per delay and distance were established. Rock properties such as compressive strength, tensile strength, shear strength, and density were determined in the laboratory. The influences of rock properties on ground vibration from blasting are presented.

INTRODUCTION

Ground vibration induced by blasting may cause structural damage and human annoyance. The intensity of ground vibration is measured in terms of peak particle velocity (PPV) in order to study and evaluate its damage potential to man and environment. PPV is related with charge weight and distance by a power function of the form $V = K(D/\sqrt{W})^n$, where V is the peak particle velocity (mm/s), D is the distance of vibration measurement from the blast (m) and W is the charge weight per delay (kg). The term $D/\sqrt{W}$ is termed the scaled distance ($m/kg^{1/2}$). K and n are site constants which vary from site to site. The variation in site constants can be attributed to different rock-mass properties at different sites. Gupta et al. [1] have reported on the influence of joints on ground vibration induced by blasting in which an attempt was made to correlate PPV with rock-quality designation (RQD) and rock-mass quality (Q). An attempt has been made

by the authors to correlate ground vibration with rock properties such as compressive strength, tensile strength and density.

METHOD

Ground vibrations were recorded during production blasts at twelve sites including opencast coal mines, limestone quarries and civil engineering hydroelectric projects. At each site, vibration was recorded with seismographs and vibration meters for varying distances from the source. Propagation equations of blast vibrations were derived by the least-square method of regression analysis and the values of K and n were computed. The constant K varied from 13.39 to 483.02 and the constant n from 0.68 to 1.89 (Table 1).

Rock samples were collected from each site and their compressive, tensile and shear strengths, and their Young's modulus, Poisson's ratio and density were determined in the laboratory. Compressive strength varies from 30 to 214 MPa, tensile strength from 2.47 to 14.61 MPa, and density from 2000 to 2860 kg/m^3. The details of rock properties and site constants for the corresponding sites are also given in Table 1.

TABLE 1

Physical and mechanical properties of rocks and corresponding site constants for various mining and civil engineering project sites

Location	Rock	Compressive strength (MPa)	Tensile strength (MPa)	Shear strength (MPa)	Density (kg/m^3)	Young's modulus (GPa)	Poisson's ratio	Site constants	
								K	n
Lambidhar mining project, Mussoorie	Grey marble	73.33	6.96	10.19	2480	–	–	129.31	−1.39
Karankote limestone quarry, Tandur, CCI	Limestone	214.02	10.58	19.80	2660	37.0	–	154.28	−1.38
Nayagaon limestone quarry, CCI	Limestone	149.61	14.61	18.82	2670	37.0	–	65.03	−0.68
Damodar OCP, Sudamdih, BCCL	Sandstone	78.14	4.31	–	2560	16.66	–	360.6	−1.89
Yerraguntala limestone quarry, CCI	Limestone	127.94	8.92	20.19	2680	18.2	–	162.97	−1.15
Bhimsagar Dam, Rajasthan	Sandstone	139.10	9.15	–	2500	–	–	181.56	−0.97
North Koel hydroelectric project, Bihar	Granitic	141.11	6.62	–	2500	–	–	483.02	−1.56
West Mudidih, OCP, BCCL	Sandstone	30.00	3.26	–	2340	–	–	286.34	−1.25
Gopinathpur, OCP, ECL	Sandstone	18.92	2.47	–	2200	–	–	292.45	−1.5
Kargali colliery, quarry No. 3, ECL	Sandstone	33.33	9.31	–	2000	–	–	324.79	−1.23
Salal hydroelectric project, J&K	Dolomite	96.08	–	–	2860	40.7	0.35	174.58	−1.51
Narmada hydroelectric project, MP	Basalt	121.50	–	–	2700	–	0.21	13.39	−0.76

INFLUENCE OF ROCK PROPERTIES ON SITE CONSTANTS

Plots of K against compressive strength, tensile strength and density are shown in Fig. 1. The data are widely scattered, indicating that the compressive and the tensile strengths are not the dominant factors which affect K. It might possibly be influenced by other parameters such as geological discontinuities, explosive properties, blast geometry and delay interval. Similarly, the attenuation constant, n, which shows decay of vibration amplitudes with distance, does not fit well with compressive and tensile strengths. The constant n also depends on the types of waves produced, body waves attenuate faster than surface waves. It also depends on frequency and orientation of joints. For this reason, plots of n against rock properties do not yield useful information.

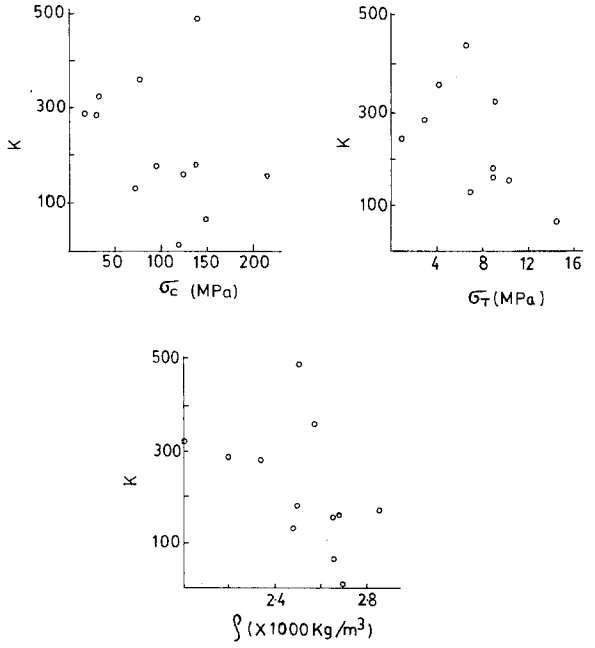

Fig. 1. Site constant K versus compressive strength σ_c, tensile strength σ_T and density ρ.

INFLUENCE OF ROCK PROPERTIES ON PPV

Peak particle velocities were computed from the propagation equation for scaled distances of 10, 20, 60 and 100 ($m/kg^{1/2}$). Plots of PPV against compressive strength of rocks for different scaled distances are shown in Fig. 2.The majority of the data indicates a general trend of PPV increasing with an increase in compressive strength. This trend at low scaled distances is not as pronounced as at greater scaled distances.

The relationship between PPV and the tensile strength of rocks is shown in Fig. 3. No definite trend is apparent at scaled distances of 10 and 20. However, at scaled distances of 60 and 100, PPV tends to increase with the tensile strength.

Compressive as well as tensile strength shows a better relationship with PPV at greater scaled distances. At lower scaled distances, particularly at smaller distances from the blast, PPV appears to be influenced more

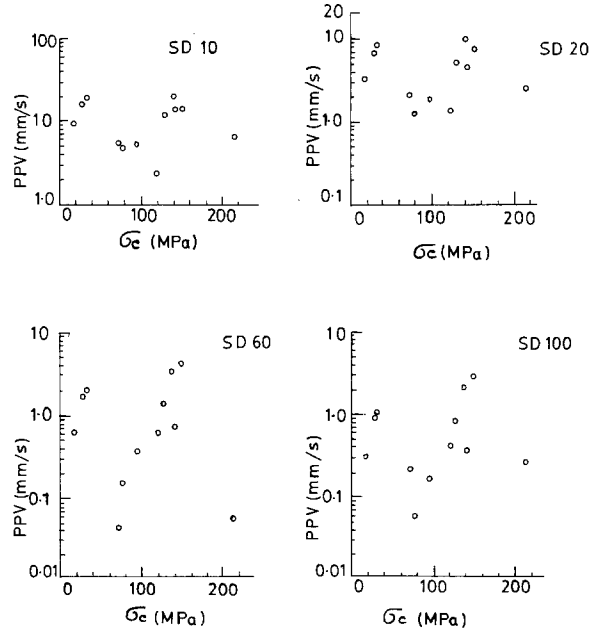

Fig. 2. Peak particle velocity versus compressive strength σ_c for different scaled distances.

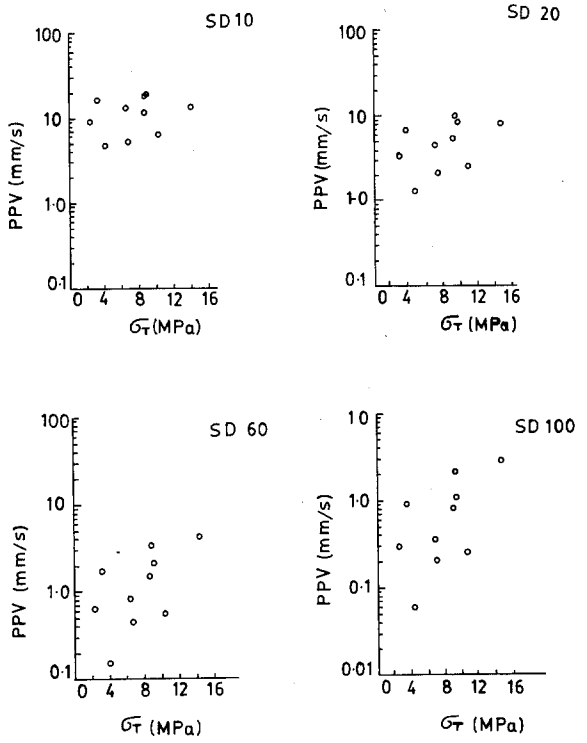

Fig. 3. Peak particle velocity versus tensile strength σ_T for different scaled distances.

by blasting pattern. The influence of strength properties on PPV becomes more pronounced as ground vibration propagates away from the blast. However, even if PPV can be predicted for greater scaled distances, it has less practical utility because the magnitude becomes within safe limits at scaled distances greater than 20. Propagation of ground vibration through a rock mass is very complex and it is difficult to establish a simple relationship between PPV and rock properties.

CONCLUSION

The following conclusions can be drawn from this study:

(1) The relationship between site constants and rock properties such as compressive and tensile strengths, and density is poor.

(2) Peak particle velocity increases with an increase in compressive as well as tensile strength. The correlation is better with compressive strength and more pronounced at greater scaled distances.

(3) An integrated approach incorporating structural discontinuities and rock properties covering a larger mass of data may produce a better relationship. Investigation is in progress.

ACKNOWLEDGEMENTS

Field investigations for this study were carried out at various mining and civil engineering project sites. The cooperation of the operators of these sites during the investigation is gratefully acknowledged. The authors express their thanks to the Director of the CMRS for permission to publish this paper.

REFERENCE

1 Gupta, R.N., Singh, M.M. and Singh, B. Influence of joints on ground vibration. In: Nat. Semin. Min.—Present and Future. Banaras Hindu Univ., Varanasi (1985).

Mining Science and Technology, 11 (1990) 173–177
Elsevier Science Publishers B.V., Amsterdam

Control of fines through blasting design at a limestone quarry

G.R. Adhikari, B.K. Barman and B. Singh
Central Mining Research Station, Dhanbad-826001 (India)

(Received August 24, 1989; accepted March 1, 1990)

ABSTRACT

Adhikari, G.R., Barman, B.K. and Singh, B., 1990. Control of fines through blasting design at a limestone quarry. Min. Sci. Technol., 11: 173–177.

Given in the paper are the results of experimental blasts in a limestone quarry for control of production of fines. The study indicated that fines can be kept to a minimum by reducing the charge factor to an optimum value, and by adopting a particular blasthole geometry. However, geological features imposed a limit on the reduction of fines.

Introduction

Lambidhar limestone quarry produces high grade limestone and marble. The materials are either classified visually as fines (particles smaller than 25 mm) and lumps or screened into different sizes. As the price of lumps is two to four times that of fines, emphasis is placed on controlling the production of fines.

The Central Mining Research Station, Dhanbad, conducted field studies to suggest suitable blasting techniques to minimize the production of fines and to control ground vibration and noise [1]. This paper describes the experimental blasts conducted at the quarry with their results. It also focuses on geological and structural influences on the production of fines.

Site geology

The deposit is made up of a major anticline which is flanked on the north and south by complimentary synclines. Marble occurs in two limbs of the anticline. Basal dolomitic limestone forms the core of the anticline. Due to tectonic disturbances the deposit is highly jointed. Four major sets of joints are encountered in the quarry faces. The orientation of the joints and modal spacing for each set are given in Table 1.

The rock mass is divided into natural blocks by intersecting discontinuities. The number of joints per m^3 at the site is 18–20, which indicates that small blocks are present in the rock mass. Not only major joints but also micro-joints are very common and well developed throughout the rock mass. The intensity of micro-jointing was assessed by counting

TABLE 1

Orientation and spacing of joints

Joint set	Dip amount (degrees)	Dip direction (degrees)	Modal spacing (m)
J_1	78	212	0.16
J_2	45	55	0.22
J_3	34	118	0.31
J_4	76	300	0.24

the number of micro-joints over a certain area. The number of micro-joints measured at the bench faces varied from 5 to 14 per 100 cm^2. The presence of these divides the natural blocks into even smaller pieces.

To ascertain the effectiveness of blast design, the experiments were conducted in grey marble at a bench level of 1970 m. Due to local variations in the nature of rock, experiments were carried out at two sites (called A and B). At site A the rock is finely crystallized grey marble. The compressive strength of the rock is 73 MPa. Grey marble being chemically active, forms a solution with rain water. The solution fills all the major- and micro-joints and behaves as a cementing material. The natural blocks are bonded together by this. The phenomenon is common only on the exposed surfaces. The rock at site B is an altered form of the grey marble encountered at site A. On the basis of joint data, fines present in-situ are estimated to be between 20 and 30%, and less than 10% at sites A and B, respectively.

Experimental procedure

Blastholes were drilled on a burden of 2.8–4.0 m and a spacing of 3.5–4.5 m. The diameter of holes was 100 mm. The depth of holes varied between 6.1 and 7.5 m and the stemming column varied from 1.2 to 3.3 m. Blasts were conducted with ANFO or slurry explosives. The charge factor varied over a wide range i.e. from 0.25 to 0.52 kg/m^3. Holes in the same row were detonated simultaneously. The delay between the rows in blast number 5 was 50 ms. The details of blasting patterns are given in Table 2.

The amount of fines produced after the blast was assessed by screening representative samples from the muckpile. The weight of samples taken was proportional to the size of

TABLE 2

Details of experimental blasts

Blast No. **	No. of holes	Depth of holes (m)	Burden (m)	Spacing (m)	Explosive used	Stemming column (m)	Charge factor kg/m^3	Remarks
1	2	7.5	3.5	4.5	Indoboost * Indomix *	2.6	0.25	Breakage not satisfactory
2	2	6.2	3.4	4.2	Indoboost Indomix	3.0	0.25	Rock was broken, displacement not satisfactory
3	2	6.1	4.0	4.2	Indoboost ANFO	1.6	0.32	One hole was broken satisfactorily other did not work well
4	4	6.2	3.4	4.2	Indoboost	1.4	0.37	Throw slightly larger
5	10	4.2	2.8	3.5	Indoboost ANFO Indomix	1.2	0.52	Excessive throw, more fines
6	2	7	3.0	4.0	Indoboost	3.0	0.30	Satisfactory throw, larger portion of lumps
7	2	6.2	3.5	4.5	Indoboost	3.3	0.30	Throw satisfactory but boulders produced.

* slurry explosives.

** Blast Nos. 1 to 5 were conducted at site A; 6 and 7 at site B.

fragments. Samples were transported to the screening site where they were reduced further by cone and quartering method. A few large size fragments which could not be fed into the screen were sorted out manually and their weights were determined. An electrically driven rotating screening machine was used for fragment size analysis. Four different fractions (0–5, 5–15, 15–25 and +25 mm) were obtained from the material flowing through the rotating drum. These fractions were weighed separately in a 200 kg spring balance and the weights were recorded.

Results

Due to the highly fractured nature of the rock a few drilling problems, such as jamming of drill rods, were experienced. Five blasts were conducted at site A and two at site B. Five blasts, including four from site A and one from site B, were analysed for production of fines and lumps. Fragmentation at site A was small. About 1 t of material was screened. As fragmentation was larger at site B, the weight of sample was 4.87 t. Fines and lumps produced during experimental blasts are shown in Fig. 1. The percentage of fines at site A varied from 33 to 64. Improvement in fragmentation can be seen from Figs. 2 and 3.

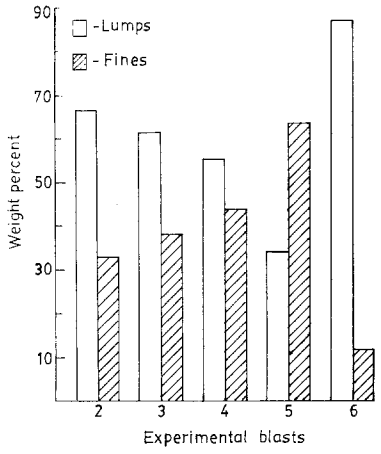

Fig. 1. Amount of fines and lumps produced during experimental blasts.

Fig. 2. Fragmentation at a charge factor of 0.37 kg/m^3.

Analysis

When an explosive detonates, two types of energy (shock and gas energy) are produced. Shock energy is responsible for creating fines while gas energy is responsible for maximum cracking and fragmentation. The zone of crushing which is formed immediately around the charge is a major source of fines due to blasting. Fines can be reduced by increasing the decoupling ratio [2], defined as the ratio of hole diameter to charge diameter. The experiments were performed with a decoupling

Fig 3. Fragmentation at a charge factor of 0.32 kg/m^3.

ratio of 1.2. Taking into consideration the availability of the type and size of the drill, and based on the work of Efremov et al. [3] in which it was demonstrated that a variation in the hole diameter did not influence the productions of fines in the zone of crushing, a hole diameter of 100 mm was used.

Based on the results of experimental blasts the most suitable pattern of blasting for the site concerned is given in Table 3. An increase in the burden and decrease in the hole spacing lead to more fines. The depth of holes depends on the bench height and subgrade drilling. At lower subgrade drilling toe problems occur while at higher, more fines would be produced due to overconfinement of gas pressure. However, the burden, spacing and hole depth could not be varied greatly because of limitations due to the bench geometry and also because unsatisfactory blasts are always frowned upon by the management. The charge factor was studied in some detail. The influence of charge factor on weight percent of fines and lumps is shown in Fig. 4. It can be seen that the amount of fines could be reduced by decreasing the charge factor to an optimum value. Rock would not be broken satisfactorily at a charge factor lower than the optimum. A higher charge factor would result in an excessive throw and production of fines up to 64.4%. At an optimum charge factor,

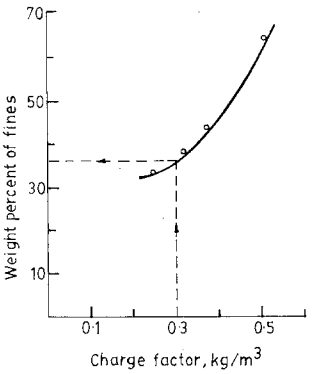

Fig. 4. Influence of charge factor on production of fines.

which was 0.3 kg/m^3 for the site concerned, fines could be minimised to 36.5%.

If rock is adequately broken in-situ, it does not require an explosive to fragment it further. All that an explosive has to do is to wedge apart the geological discontinuities by the gas pressure and displace the material slightly. Due to the nature of the rock and dry borehole conditions, ANFO was found suitable for blasting at the quarry. It was recommended that explosives should be used in cartridge form to provide a decoupling ratio of 1.2–1.25.

Judging by the compressive strength of the grey marble, which is high, there was no other reason for excessive fines except the joint structure. A comparative study of fines produced after blasting at sites A and B shows that the fines present in the rock mass before blasting had a significant influence on blasting results. At site A, where the estimated fines in-situ were 20–30%, modification of blasting design did not permit their reduction below 35%. At site B, where in-situ blocks are interlocked by cementing material, fines could be reduced to 12%. Thus, the percentage of fines present in the rock mass before blasting imposes limitations on reduction of fines with modification of the blasting pattern. The results of this study agree well with the work of La Pointe and Ganow [4].

TABLE 3

Recommended blasting parameters

Parameter	Recommendation
Hole diameter	100 mm
Bench height	6–7 m
Burden	3 m
Spacing	4 m
Depth of holes	6.5–7.5 m
Stemming column	2.8–3.2 m
Charge factor	0.30 kg/m^3
Explosive to be used	ANFO as main charge Indoboost as primer charge

Conclusion

From the blasting experiments at Lambidhar limestone quarry it may be concluded that the recommended pattern of blasting would help minimize the production of fines. However, minimization of fines will depend on the percentage of fines already present due to jointing or micro-jointing. Although reduction of fines may be achieved by adopting the optimum charge factor for a given site, the authors feel the need for further research to establish general relations between the production of fines and all variables influencing this; i.e., burden, hole spacing, hole depth, charge factor and degree of jointing. Before embarking on such a research programme, however, the practical difficulties of screening and weighing and the limitations imposed by the bench geometry should be realised. It was because of these difficulties that the investigations in this paper could not be more comprehensive.

Acknowledgement

The authors wish to thank their colleague Dr. P.R. Sheorey for his help in preparing this paper.

References

1 Anon., Blasting studies at Lambidhar limestone quarry of UPSMDC to reduce the production of fines and to control ground vibration and noise. Cent. Min. Res. Stn. Rep. MT/PF/14/87 (1988) (unpubl.).
2 Konya, C.J., Britton, R. and Lukovic, S., Charge decoupling and its effect on energy release and transmission for one dynamite and water gel explosive. Proc. Mini-symp. Explos. Blasting Res., 3rd (Miami, Fla.). Soc. Explos. Eng. (1987), pp. 14–25.
3 Efremov, E.I., Usik, I.N., Petrenko, V.D. and Usik, I.I., Breaking solid bodies by charges of different diameters. Sov. Min. J., 1 (3) (1987): 83–88 (translated from Izv. Vyssh. Uchebn. Zaved. Gorn. Zh., 9 (1987): 56–63).
4 La Pointe, P.R. and Ganow, H.G., The influence of cleats and joints on production blast fragment size in the Wyodak Coal, Compbell Country, Wyoming. Proc. U.S. Symp. Rock Mech., 27th (Univ. Alabama). (1986), pp. 464–470.